Reexamination of the Tropical Cyclone Wind–Pressure Relationship Based on Pre-1987 Aircraft Data in the Western North Pacific

LINA BAI AND HUI YU

Shanghai Typhoon Institute, CMA, Shanghai, China

PETER G. BLACK

NOAA/NCEP Environmental Modeling Center, I.M. Systems Group, College Park, Maryland

YINGLONG XU

National Meteorological Center, CMA, Beijing, China

MING YING, JIE TANG, AND RONG GUO

Shanghai Typhoon Institute, CMA, Shanghai, China

(Manuscript received 4 January 2018, in final form 27 September 2019)

ABSTRACT

The wind–pressure relationship (WPR) for tropical cyclones (TCs) in the western North Pacific is reexamined based on aircraft data, TC best track data, and daily reanalysis data during 1957–87. Minimum sea level pressure (MSLP) was estimated from aircraft reconnaissance, and maximum surface wind speeds (MSWs) were adjusted from the maximum wind speed at flight level. The mean MSLP was found to be higher during 1957–64 than during 1965–87, presumably due to the change in reconnaissance instrumentation and technology, which results in a systematic MSW bias (too high) before 1965 in the China Meteorological Administration (CMA) dataset. Further analyses found that the WPR used in the CMA dataset is more accurate for strong TCs, while the WPR in the Tokyo Regional Specialized Meteorological Center (RSMC) dataset is better for weak TCs after the MSW-RSMC converted by the Dvorak conversion table (1984) and when using the aircraft datasets as a baseline. Several prevailing operational WPRs used in the western North Pacific are reexamined. Results show that the WPR of Knaff and Zehr explains 71% of the variance with a MAE of 9.22 hPa, which represents a significant improvement over other WPRs. Utilizing data after 1965 (a total of 1874 samples), the effects of TC center latitude, size, translation speed, intensification trend, and environmental pressure on the WPRs were examined. Results show that faster-traveling TCs, smaller in size, and located in a higher environmental pressure at lower latitudes, exhibited a higher MSLP for a given MSW. Meanwhile, the latitude, translational speed, and the environmental pressure produces additional improvement, but the TC size and intensity change added only a little skill to the WPR equation.

1. Introduction

Tropical cyclone (TC) intensity is defined by the minimum sea level pressure (MSLP) and the maximum surface wind speed (MSW) measured at a standard 10-m height near the TC center. However, in open ocean regions, there are sparse direct TC observations. Prior to 1987, the MSLP was commonly measured using dropsondes deployed during aircraft reconnaissance or extrapolated to the surface from the flight altitude height in the western North Pacific (WNP). The MSW is estimated by adjusting the wind speeds at flight level, or by using a wind–pressure relationship (WPR). After 1987, satellite data of continuously increasing resolution and coverage have been utilized in the WNP when

Denotes content that is immediately available upon publication as open access.

Corresponding author: Bai Lina, bailn@typhoon.org.cn

DOI: 10.1175/WAF-D-18-0002.1

aircraft observations have been unavailable. The Dvorak approach (Dvorak 1975, 1984; Velden et al. 2006), widely used for decades, applies a pattern recognition technique that extracts satellite features to derive an estimate of either the MSLP or MSW, and a WPR is then used to estimate the other variable. Therefore, the WPR is essential to operational forecasts and climate research (Knaff and Sampson 2006; Knapp et al. 2013).

Various WPRs have been developed in recent decades. Several were obtained by compositing observational data of the MSW and MSLP. In addition to the development of the TC intensity estimation technique based on satellite imagery, Dvorak (1975, 1984) also proposed an empirical relationship between the current intensity (CI) number, MSW, and MSLP. This has been employed in some operational centers such as the National Hurricane Center/Tropical Prediction Center (Knaff and Zehr 2007). A similar WPR reported by Koba et al. (1991) also detailed the relationships between the same three parameters, which was used by the Tokyo Regional Specialized Meteorological Center (RSMC).

Some earlier WPRs were derived based on the cyclostrophic wind equation:

$$\frac{1}{\rho}\frac{\partial p}{\partial r}=\frac{V_t^2}{r}, \tag{1}$$

where V_t is the tangential wind, r is the radius, p is pressure, and ρ is density. Several approximations (e.g., ρ is assumed to be constant, and the pressure in the radius of MSW is equal to the environmental pressure) were applied in the integral term of Eq. (1). Subsequently, the practical form of the WPR was given by

$$\mathrm{MSW}=a(p_{\mathrm{env}}-\mathrm{MSLP})^n, \tag{2}$$

where p_{env} is the environmental pressure, and a and n are empirical constants. The relationships were improved periodically by varying the values of a and n (Takahashi 1939, 1952; Fortner 1958; Atkinson and Holliday 1977; Love and Murphy 1985; Black 1993; Harper 2002). The most widely used relationship in the WNP was that derived by Atkinson and Holliday (1977) given by

$$\mathrm{MSW}=3.4(1010-\mathrm{MSLP})^{0.644}. \tag{3}$$

It is likely that the WPR is influenced by variable parameters; therefore, several WPRs have been developed by first binning data into subsets of latitudinal and sizes before building a best fit (Harper 2002). For example, the WPR for the TC best track data of the China Meteorological Administration (CMA) during 1949–71 was a set of latitude-dependent regression equations based on in situ observations (Ying et al. 2014). Most recently, a new WPR based on the cyclostrophic wind equation was presented by Holland (2008). The final form of the WPR was given by

$$\mathrm{MSW}=\left(\frac{b_s}{\rho e}\Delta p\right)^{0.5}, \tag{4}$$

where $\Delta p = p_{\mathrm{env}} - \mathrm{MSLP}$, e is the base of natural logarithms, ρ is surface air density, $b_s=-4.4\times10^{-5}\Delta p^2+0.01\Delta p+0.03(\partial p_c/\partial t)-0.014\varphi+0.15v_t^x+1.0$, which indicates the variation of the pressure gradient near the radius of MSW, varying with Δp, intensification trend $\partial p_c/\partial t$, latitude φ, and moving speed v_t.

Previous studies suggested that the gradient wind balance provides a better approximation of the core of a TC (Willoughby 1990; Willoughby and Rahn 2004) such that

$$\frac{1}{\rho}\frac{\partial p}{\partial r}=\frac{V_t^2}{r}+fV_t, \tag{5}$$

where f is the Coriolis parameter, given by $f=2\Omega\sin\varphi$. The three terms of Eq. (5) indicate the pressure gradient force, centrifugal force and Coriolis force, respectively. The integration of Eq. (5) yields the following:

$$\mathrm{MSLP}=P_{\mathrm{env}}-\int_{r=0}^{r_{\mathrm{env}}}\rho\left(\frac{V_t^2}{r}+fV_t\right)dr, \tag{6}$$

where r_{env} is the radius of the environmental pressure P_{env}. Using predictors that are associated with Eq. (6), Knaff and Zehr (2007) developed a unified method by using the least squares best fit of various parameters on the WPR. The method considered the effect of TC size, latitude, translation speed, and environmental pressure on the WPR such that

$$\mathrm{MSLP}=23.286-0.483V_{\mathrm{srm}}-\left(\frac{V_{\mathrm{srm}}}{24.254}\right)^2-12.587S-0.483\varphi+p_{\mathrm{env}}, \tag{7}$$

where is V_{srm} is the maximum wind with translation speed removed (Schwerdt et al. 1979), and S is TC size. The relationships developed by Knaff and Zehr (2007) could be considered better than traditional WPRs. Courtney and Knaff (2009) developed a modified version of Knaff and Zehr's (2007) WPR, which estimated size from the mean radius of gales, since 34-kt

(1 kt $\approx$ 0.51 m s^{-1}) wind radii are a routine operational estimate at BoM and NOAA (NHC, CPHC) and JTWC. The WPR developed by Atkinson and Holliday (1977) was a primary TC intensity determination tool used for JTWC operations during 1978–2006. The Atkinson and Holliday (1977) WPR has been replaced by Knaff and Zehr's (2007) WPR for operational use at JTWC since 2007 (U.S. Fleet Weather Facility 2007).

More recently, Kieu et al. (2010) examined the dynamical constraints for intense TCs, and suggested that the TC tendency and frictional forcing are important for intense TCs with a small eye size. They hypothesized a simple nonlinear form of the WPR that incorporated the centrifugal effect, Coriolis forcing, intensification trend, and frictional forcing. Overall, they suggested a modified version of the statistical WPR given by

$$\begin{aligned}\mathrm{MSLP} - P_{\mathrm{env}} = {} & a_0 + a_1\mathrm{MSW} + a_2 S + a_3\varphi + a_4\frac{\partial \mathrm{MSW}}{\partial t} \\ & + a_5\mathrm{MSW}^2 + a_6\frac{\partial \mathrm{MSW}}{\partial t}\times S \\ & + a_7\mathrm{MSW}\times S, \end{aligned} \tag{8}$$

suggesting that the TC size should be coupled with MSW, and the TC tendency ∂MSW/∂t should be considered with the TC size, rather than used independently. Chavas et al. (2017) tested the fundamental physical relationship between the central pressure deficit and its wind field via gradient wind balance. Their results showed that the pressure deficit is physically a function of MSW, and half the product of the Coriolis parameter and a measure of outer storm size.

Although recent statistical WPRs, such as those developed by Knaff and Zehr (2007), Holland (2008), and Courtney and Knaff (2009), show improvement over earlier WPRs, several issues remain that need addressing. First, the Knaff and Zehr (2007) WPR was developed with the use of MSW interpolated from best track data in the Atlantic and eastern and central North Pacific. Holland (2008) chose the North Atlantic HURDAT data to develop their WPR. However, aircraft reconnaissance is available in the WNP during 1949–87 that provides flight-level winds, surface winds, and MSLP independently. Therefore, WPRs derived using such aircraft data can provide additional independent information for the WNP. Second, studies have shown factors affecting the WPR include TC center latitude, size, translation speed, intensification trend, environmental pressure, and the radial wind (Schwerdt et al. 1979; Koba et al. 1991; Knaff and Zehr 2007; Holland 2008; Kieu et al. 2010). The parametric WPR model of Knaff and Zehr (2007) considered the linear effects of TC center latitude, TC size, and environmental pressure, but not their coupled effects. Kieu et al. (2010) proposed a nonlinear form of the WPR, which also considered the coupled effects of $(\partial V/\partial t) \times S$ and MSW $\times S$ on Δp. Chavas et al. (2017) found that the Δp is physically a function of $(1/2)f \times S$ and MSW. Therefore, there is a need to compare the effect of these linear and nonlinear factors on WPR.

This paper will compare the WPRs based on aircraft observations before 1987 with WPR of best track data, and reexamine several prevailing operational WPRs used in WNP. Then the effects of several factors (i.e., TC size, environmental pressure, latitude, TC motion, and intensification trend) on the WPR are also discussed.

2. Datasets and methodology

Aircraft reconnaissance reports in the WNP during 1949–87 were documented in the CMA Typhoon Yearbook. The aircraft observations in the WNP began in 1943 (Henderson 1978); however, there were a greater number of routine reconnaissance flights after 1956 due to the increase in the number of aircraft with improved navigational equipment that employed automatic data recording systems (Laseur and Hawkins 1963). In addition, the aircraft and the Doppler wind navigational instruments onboard were upgraded in the middle and late 1960s (U.S. Fleet Weather Facility 1965; Weatherford and Gray 1988). Further details on the aircraft reconnaissance are provided by Henderson (1978).

During the surveys, each aircraft fix records a time, location, flight altitude, MSLP, the maximum winds at flight level (MFW), and MSWs. In general, the MSLP was obtained directly from dropsondes, or extrapolated to the surface from 700-hPa geopotential height based on a regression equation (Willoughby et al. 1989). The second computing method of MSLP became the chief way since 1978 (U.S. Fleet Weather Facility 1978), with errors of 4–5 hPa (Atkinson and Holliday 1977; Knapp et al. 2013). The MSWs were estimated subjectively by the Aerial Weather Reconnaissance Officers based on the general appearance of the ocean surface when observable. Sometimes the MSWs were estimated via the MSLP, since the sea state was difficult to be observed, particularly at night. Errors in the MSWs' estimation increased at high wind speeds (Operational Department of China Central Meteorological Administration 1980; Neumann 1952) and are categorized in the following way. For wind speeds less than 25 m s^{-1}, the error was

$\sim$5 m s^{-1}. For wind speeds that reached 38 or 50 m s^{-1}, the error increased to 5–10 and 8–10 m s^{-1}, respectively. For wind speeds above 75 m s^{-1}, the error exceeded 13 m s^{-1}. The MFW was observed by Doppler radar with high precision, and the mean error of a moving surface for Doppler equipment was $\sim$1.5 m s^{-1} (Grocott 1963; Operational Department of China Central Meteorological Administration 1980).

Figure 1 shows the flight altitude and MFW from all aircraft observations during 1957–64 and 1965–87. In general, the aircraft reconnaissance observations are obtained from three relative safety levels: flight altitudes below 900 hPa in weaker TCs, altitudes around 700 hPa, and higher altitudes around 500 hPa. Franklin et al. (2003) recommended the wind adjustment factors for adjusting flight-level winds to the surface for the eyewall regions of TCs, which are 0.9, 0.8, and 0.75 for 700, 850, and 925 hPa, respectively. In this study, the MSW is determined from the MFW at 700 hPa by employing the recommended ratio (i.e., 0.9). In addition, to obtain robust results based on extensive data for this step, samples at 650–750-hPa flight levels (N = 3944) were chosen.

The next step involves a comparison of the MSW derived from the flight-level wind speed with the MSWs. Samples were included when the difference between MSW and MSWs was less than the error of the MSWs estimation. That is, the difference should be less than 5, 10, and 13 m s^{-1} when the MSW is <25, 25–50, and >50 m s^{-1}, respectively. The screening sequence resulted in 2677 samples being used in this study. As shown in Fig. 2, the geographic locations of the selected samples span a wide region of the ocean (i.e., 4.0°–43.6°N, 100.5°–179.7°E).

The latitude of the TC center φ is obtained directly from the aircraft data. TC translation speed (SPD) and intensification trend V_t over the previous 12 h are calculated from CMA best track data. The MSW and TC center locations are interpolated onto the current and 12-h-prior aircraft fix time using 6-hourly values from the best track data. Subsequently, the intensity change V_t and SPD are calculated. Environmental sea level pressure P_{env} and TC size are estimated based on the Japanese 55-year Reanalysis (JRA-55), using daily 3-hourly data from the Japan Meteorological Agency. The environmental pressure is averaged within an 800–1000-km annulus surrounding the TC center. Here, the TC size is defined using two variables. The first is the mean radius of 8 m s^{-1} surface winds (herein S_8), which is considered as the outer TC size. The calculation of S_8 is suggested by Chavas et al. (2017), which is defined as the innermost wind radius beyond radius of maximum wind, and the algorithm saturates at 1500 km. Following the model of

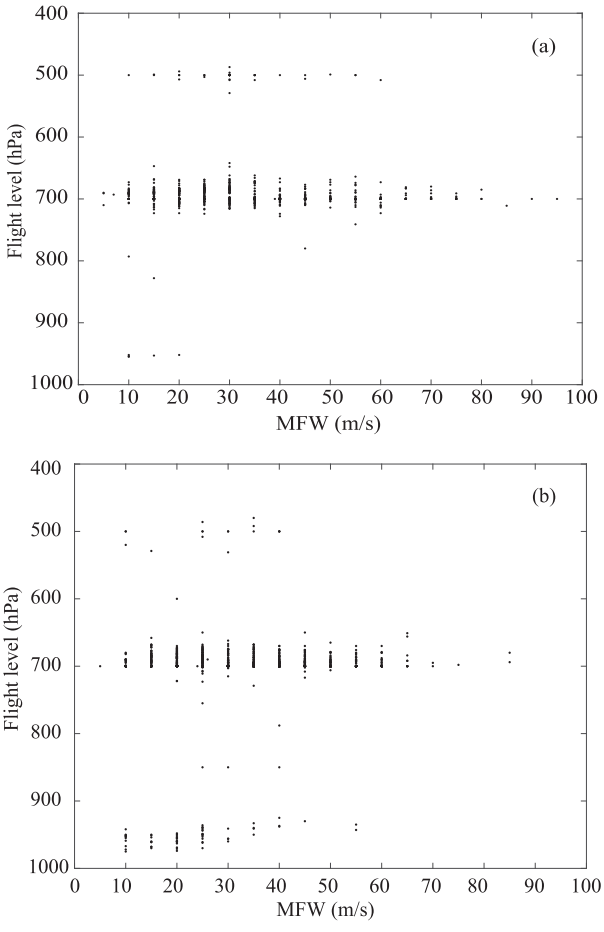

FIG. 1. Relationship between flight level and MFW from aircraft observations during (a) 1957–64 and (b) 1965–87.

Knaff and Zehr (2007), the second variable (herein S_{KZ}) is the ratio between the tangential wind at r = 500 km (V_{500}) and its climatological value at the same radius (V_{500c}). The V_{500c} is estimated from the TC latitude and MSW. The wind speeds from the JRA reanalysis data are interpolated onto a finer grid (0.1°).

3. Comparison of wind–pressure relationships based on aircraft observations and best track data

To examine whether changes in aircraft and observational instruments around 1965 affected the relationship between the MSLP and MSW, the mean MSLP for each MSW group (separated using 4.5 m s^{-1} intervals) during 1957–64 and 1965–87 was calculated (Fig. 3). An interval of 4.5 m s^{-1} was chosen for the MSW because the documented MFWs in the CMA Typhoon Yearbook are given to the nearest 5 m s^{-1}. The number of samples with MSW greater than 65 m s^{-1} was limited during the

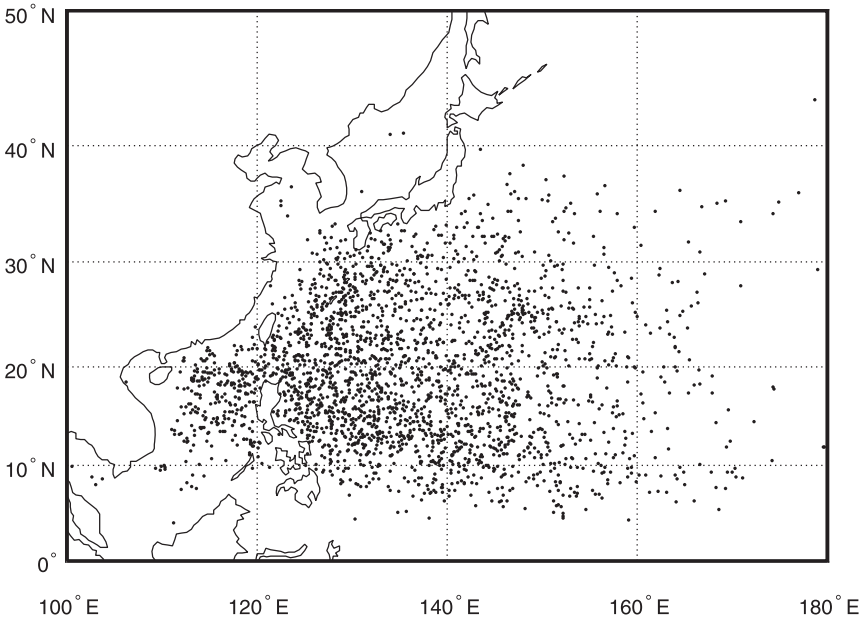

FIG. 2. Geographic locations of the individual aircraft reconnaissance fixes used in this study.

two periods (i.e., <10); consequently, such cases were combined with the previous group (i.e., ≥58.5 m s^{-1}). Results show that the MSLP decreased as the MSW increased for both periods, consistent with previous studies (Harper 2002). The correlation coefficients between the MSLP and MSW for all cases are −0.87 and −0.81 for the two time periods, respectively, which exceeds the 99% level of statistical significance (F test). The correlation coefficients between the mean MSLP and MSW are −0.98 and −0.99 for the two time periods, respectively. Figure 3 also shows the MSLP is higher during 1957–64 than during 1965–87 for each MSW group, except when MSW exceeds 58.5 m s^{-1}. The mean MSLP in the first time period is 5.7 hPa larger than in the second period when the MSW is less than 58.5 m s^{-1}. The largest difference of 11.4 hPa is seen for a MSW of 54 m s^{-1}. Interestingly, the MSLP for the 58.5 m s^{-1} group is lower during 1957–64 than during 1965–87, due primarily to the mean MSW in this group being larger in the first period than in the second, with values of 62.2 and 60.9 m s^{-1}, respectively.

To determine the cause of the difference in the WPR prior to and after 1965, the annual frequencies of the MSLP and MSW are calculated (Fig. 4). The frequencies

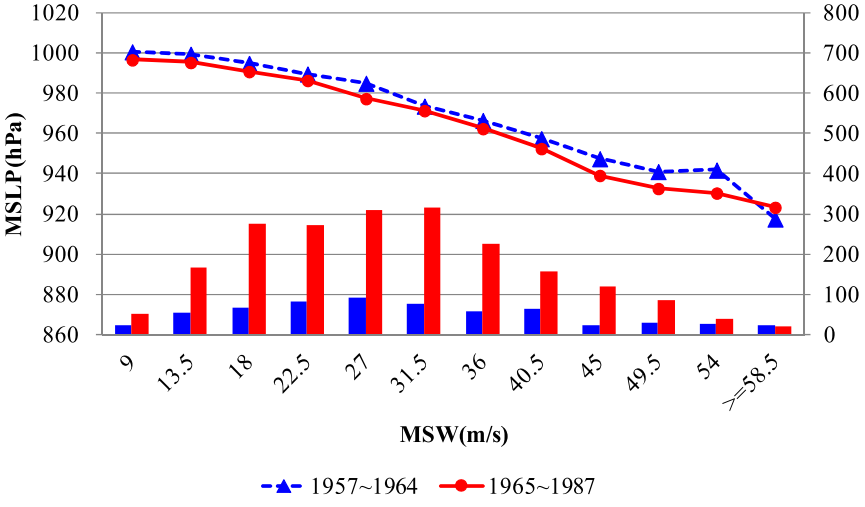

FIG. 3. Mean MSLP (lines) and number of samples (bars) for each MSW group during 1957–64 (blue triangles) and 1965–87 (red circles).

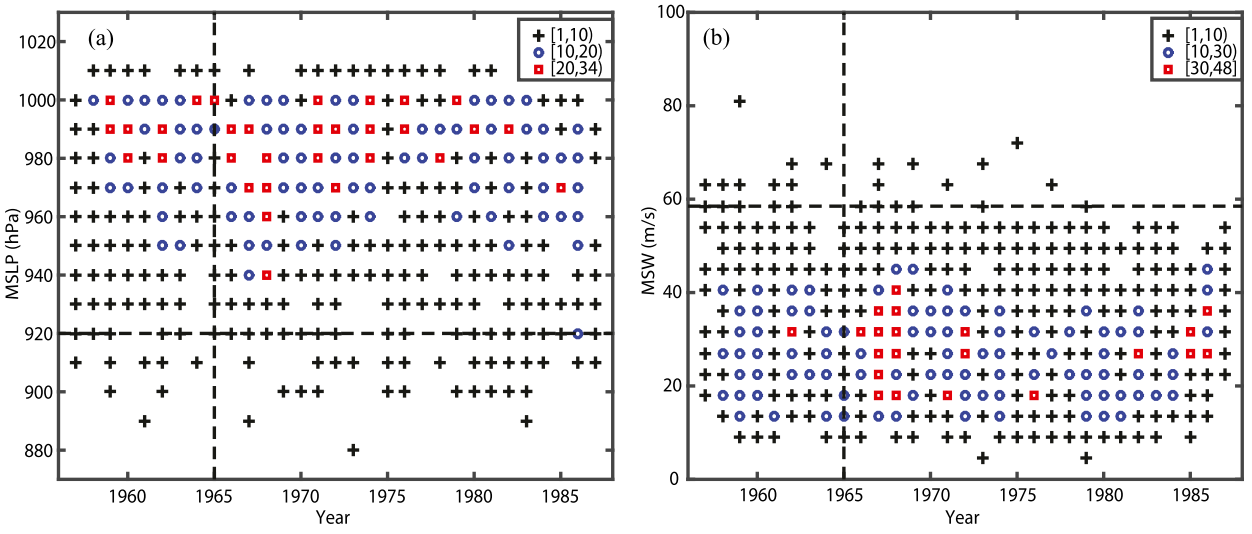

FIG. 4. Annual frequency of (a) MSLP and (b) MSW values (denoted by different symbols for each interval indicated at top right). The vertical dotted lines separate the two time periods (pre- and post-1965). In (a) and (b), the horizontal dotted lines indicate a MSLP equal to 920 hPa and a MSW equal to 58.5 m s^{-1}, respectively.

of an extreme TC intensity are compared between the two time periods. During 1957–64, the frequency of MSLP $\leq$ 920 hPa is 20 (Fig. 4a), similar to the frequency of MSW $\geq$ 58.5 m s^{-1} (i.e., 22; Fig. 4b). However, the frequency of an exceptionally low MSLP during the later time period (1965–87) is 76, which is 3.6 times the frequency of an exceptionally large MSW (i.e., 21). Overall, there is little difference in the annual frequency of low MSLP during the two periods; however, the frequency of large MSW decreased substantially during the later period. Differences in aircraft reconnaissance wind estimations may be responsible for the apparent decadal variability in the WPR during the two periods. Given the possible influence on WPR of changes in reconnaissance instrumentation and technology around 1965, only data after 1965 are used in the following analyses, totaling 1874 samples.

To compare WPR based on aircraft observations with WPR of the best track data, the comparisons between the aircraft-based records with TC best track data from CMA, and RSMC-Tokyo for 1965–87 were performed. The MSW and MSLP are interpolated onto the current aircraft fix time using 6-hourly values from the best track data. The CMA dataset including MSW and MSLP covers the entire period of record of aircraft reconnaissance. The RSMC-Tokyo has gathered the MSLP records since 1951, but MSW records only since 1977. The JTWC best track dataset does not contain MSLP records before 1987, so the comparison here does not include the JTWC dataset.

On a diagram comparing MSLP between aircraft reconnaissance (MSLP-AR) and the CMA dataset for 1965–87, the data are concentrated around the diagonal 1:1 line (Fig. 5a). The bias ranges from −6.0 hPa for samples of 1005–1015 hPa to 4.0 hPa for samples of 890–895 hPa. The mean bias is −0.6 hPa, with a correlation coefficient of 0.99. The MSLP values from the RSMC-Tokyo dataset are also consistent with aircraft-based pressure data, with a mean bias of −1.2 hPa and correlation coefficient of 0.98 (Fig. 5b).

Figure 6 compares the maximum wind report at flight level in aircraft reconnaissance records and the MSW reported in the best track data. The wind samples are scatter in a wider region around the 1:1 line than the MSLP. The wind bias between the MFW and the MSW in the CMA dataset ranges from −6.7 m s^{-1} for samples of 70 m s^{-1} MFW to 7.6 m s^{-1} for samples of 10 m s^{-1} MFW. The bias is very small (<1 m s^{-1}) for samples within 35–60 m s^{-1}. The low bias and high correlation coefficient (0.85) indicate that the estimates of the MSW in the CMA best track data are influenced by flight-level wind values in a systematic manner. The mean bias for each agency appears to diverge. The CMA data have a mean bias of +0.5 m s^{-1}, while the RSMC-Tokyo data have a negative bias of about −1.9 m s^{-1}. The divergence might arise because the MSW in each agency was averaged over different time periods: 2 min for the CMA dataset and 10 min for the RSMC-Tokyo dataset.

There are two methods to transfer 10-min average MSW-RSMC to 1-min MSW. The first method is proposed by Atkinson (1974). The MSW-RSMC is multiplied by a ratio (1/0.88), which is hereafter referred to MSW-RSMC/0.88. In recent years, several studies pointed that there is not linear relationship between 10-min and 1-min

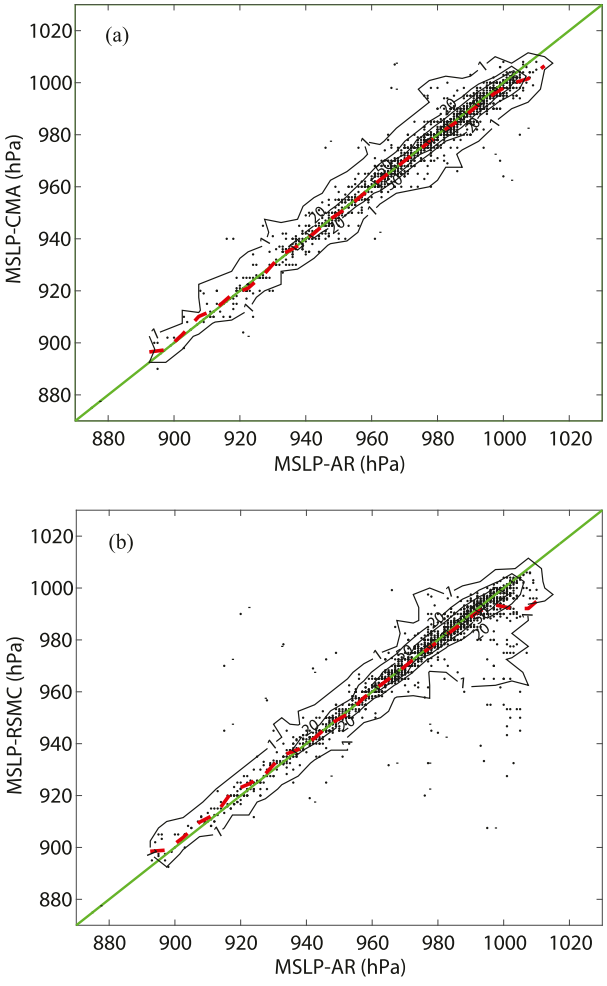

FIG. 5. Scatter diagrams of (a) MSLP-AR and MSLP-CMA during 1965–87 and (b) MLSP-AR and MSLP-RSMC during 1965–87. The green solid diagonal lines indicate that the two MSLP values are equal. The black solid lines indicate the number of samples in a 5 hPa × 5 hPa grid. The dashed lines indicate the mean values for each 5-hPa group.

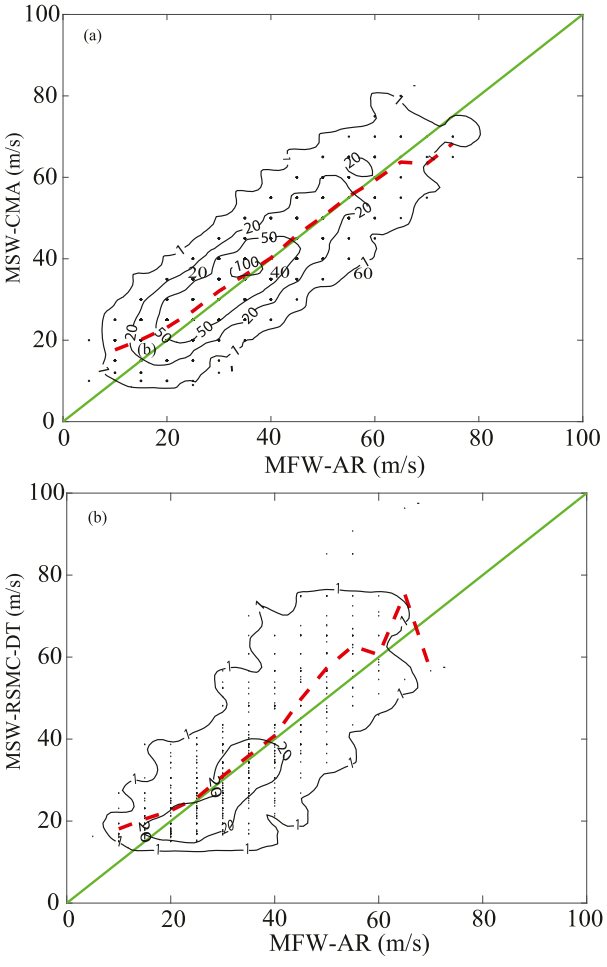

FIG. 6. Scatter diagrams of (a) MFW-AR and MSW-CMA during 1965–87 and (b) MFW-AR and MSW-RSMC-DT during 1977–87. MSW-RSMC-DT indicates the MSW-RSMC was converted based on the Dvorak conversion table (1984). The green solid diagonal lines indicate that the two MSW values are equal. The black thin lines indicate the number of samples in a 5 m s^{-1} × 5 m s^{-1} grid. The red dashed lines indicate the mean values for each 5 m s^{-1} group.

average wind speed (Knapp and Kruk 2010; Song et al. 2010). The second method was suggested by Knapp and Kruk (2010). First, the RSMC-Tokyo MSW was reverted to CI numbers based on the conversion tables suggested in Koba et al. (1991). Second, the wind speed was derived from CI numbers based on Dvorak (1984) CI-MSW conversion table. This converted MSW-RSMC (hereafter MSW-RSMC-DT) was also shown in Fig. 6. The mean bias between the MSW-RSMC-DT and the aircraft data is 2.84 m s^{-1}, with very small bias (<1 m s^{-1}) for samples within 25–40 m s^{-1}. The MSW-RSMC-DT is larger than aircraft wind data for each MFW group, except when the MFW exceeds 70 m s^{-1}. But there is not statistical meaning, since there is only one case of the MFW exceeds 70 m s^{-1}. The MSW-RSMC/0.88 is larger than MSW-RSMC-DT for MFW weaker than 45 m s^{-1}, but smaller for MFW stronger than 45 m s^{-1}.

In summary, the MSLP values from each best track dataset are consistent with the aircraft-based MSLP, and the MSW values are also influenced by flight-level wind values in a systematic manner. However, if the MSW is adjusted from the MFW based on the ratio suggested by Franklin et al. (2003), the aircraft-adjusted MSW is 10% lower than the estimates in the best track data. This result is consistent with the findings of studies in the North Atlantic (Uhlhorn and Nolan 2012; Nolan et al. 2014), because the aircraft only samples those portions of the TC along the flight path, while the flight path may

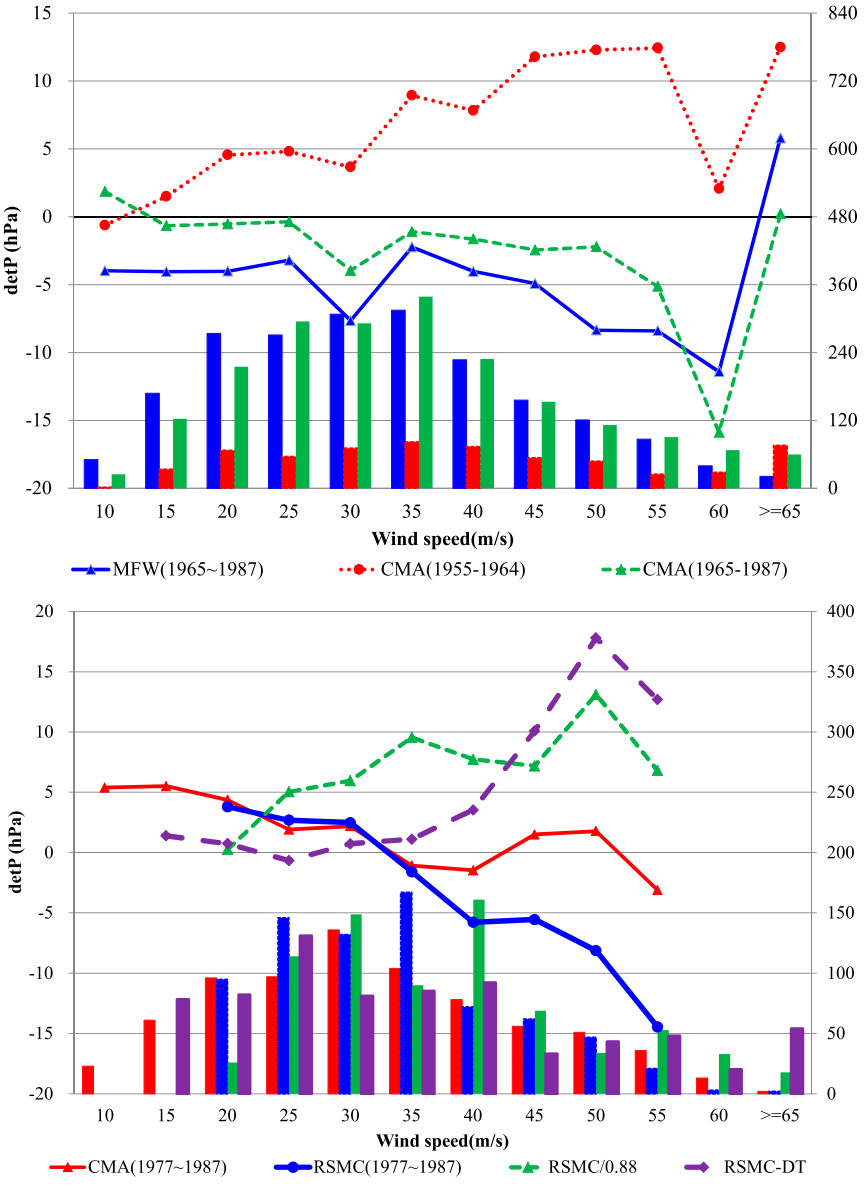

FIG. 7. (a) Mean MSLP difference (detP; lines) and number of samples (bars) for each MFW group between aircraft data during 1965–87 (blue), the CMA dataset during 1957–64 (red), and the CMA dataset during 1965–87 (green), with the aircraft data during 1957–64. (b) Mean MSLP difference (detP; lines) and number of samples (bar) for each MFW group between CMA, RSMC-Tokyo, and modified best track datasets with the aircraft data during 1977–87. RSMC/0.88 indicates the MSW of RSMC multiplied by a factor (1/0.88), and RSMC-DT indicates the MSW was converted based on the Dvorak conversion table (1984).

be not through the strongest sector of the TC in many instances.

Figure 7 shows the mean MSLP for each aircraft-estimated MFW group and the WPR based on best track datasets. The distribution of the mean MSLP for 1965–87 in the CMA datasets is similar to that in the aircraft-based datasets, whereas the MSLP for each wind group in 1955–64 is much higher based on CMA datasets than on aircraft-based datasets. This discrepancy arises from two aspects. The first one is because of the differences in aircraft reconnaissance wind estimates during the two periods. Aircraft reconnaissance datasets were the preferred source of data over the open ocean when CMA determined TC best track (Ying et al. 2014). As is stated above, the frequency of large MSW base on reconnaissance observation decreased

substantially during the later period. The second reason is that the WPR for the CMA dataset was changed during 1972. For the previous period (1949–71), the WPR for the CMA best track datasets is a set of latitude-dependent regression equations mainly based on some studies by the JTWC (Operational Department of China Central Meteorological Administration 1980; Ying et al. 2014). As Knaff and Zehr (2007) shows, the best fit of WPR in JTWC best track datasets is similar to Dvorak WPR (1975) during the period 1966–73. For the latter period (1972–present), the WPR used is based on a conversion table, which will be discussed in the next section. This CMA-WPR performed equivalently with the Atkinson and Holliday (1977) (AH) WPR. Base on the aircraft data, the CMA WPR table and AH WPR performed better than Dvorak WPR. There is an overestimation of MSW based on Dvorak WPR. Therefore, the WPR for the CMA dataset during the second time period is most similar to the observation-based WPR. There was a systematic wind speed bias (too high) before 1965 in the CMA best track dataset.

The mean MSLP for each wind speed group from the aircraft datasets, CMA, RSMC, and modified best track datasets during 1977–87 are shown in Fig. 7b. The MSLP-CMA is consistent with MSLP-AR, especially for strong TCs (MSW-CMA $\geq 35\,\mathrm{m\,s^{-1}}$), with the mean error less than 2 hPa. Figure 7b also shows that MSLP-RSMC is lower than MSLP-CMA and MSLP-AR for strong TCs (MSW $> 35\,\mathrm{m\,s^{-1}}$), but almost equal to MSLP-CMA for weak TCs (MSW $\leq 35\,\mathrm{m\,s^{-1}}$). After MSW-RSMC was converted to 1-min mean wind speed, there is a positive bias throughout the entire intensity range for the MSLP values based on MSW-RSMC/0.88. In the other way, the MSLP values based on MSW-RSMC-DT groups are consistent with MSLP-AR for weak TCs (MSW-RSMC-DT $\leq 35\,\mathrm{m\,s^{-1}}$), with the mean error less than 2 hPa, while which is higher than MSLP-AR for strong TCs.

In summary, the WPR based on the CMA best track data is more close to the aircraft-based WPR for strong TCs (MSW $\geq 35\,\mathrm{m\,s^{-1}}$). However, the WPR based on the RSMC dataset is more close to the aircraft-based WPR for weak TCs (MSW $\leq 35\,\mathrm{m\,s^{-1}}$), after the MSW-RSMC converted by the Dvorak conversion table (1984).

4. Reexamination of the prevailing wind–pressure relationships

As discussed in section 3, the aircraft-adjusted MSW is about 10% lower than what is estimated in the best track data; therefore, the aircraft MFW is adopted as the TC intensity in the following WPRs. Several operational WPRs used in the WNP are reexamined here, which include the WPRs suggested by Dvorak (1975), Koba et al. (1991), Atkinson and Holliday (1977), Knaff and Zehr (2007), and the WPR used by CMA (Ying et al. 2014). Other WPRs are suggested based on more recent physical understandings, including WPRs derived by Kieu et al. (2010) and Chavas et al. (2017). These regression models for the WPR are developed based on the samples from the period 1965–85. A set of independent samples from the period 1986–87 are used to evaluate the parametric model.

First, a gradient fit of the relationship table of Dvorak (1975) for the WNP was created as MSLP = −0.70MSW − (MSW^2/107.45) + 1015.4, which introduces an explained variance of 99.98%, a mean absolute error (MAE) of 0.69 hPa, and a bias of −0.06 hPa to the WPR table of Dvorak (1975). Similarly, the relationship table of Koba et al. (1991) was fitted to MSLP = −0.35MSW − (MSW^2/38.15) + 1013.02, where the MSW is transferred to the 1-min sustained wind speed. This function introduces an explained variance of 99.99%, a MAE of 0.44 hPa, and a bias of 0.07 hPa to the WPR table of Koba et al. (1991). Another WPR model, proposed by Atkinson and Holliday (1977), takes the form MSW = 3.447(1010 − MSLP)$^{0.644}$.

The procedure of the Knaff and Zehr (2007) WPR is repeated to obtain the coefficients of each variable based on the aircraft datasets in this paper (see the appendix). The WPR was created as follows:

$$\mathrm{MSLP} = 8.086 - 0.600V_{\mathrm{srm}} - 0.012V_{\mathrm{srm}}^2 - 3.18S_{\mathrm{KZ}} - 0.166\varphi + P_{\mathrm{env}}, \tag{9}$$

where V_{srm} is the maximum wind speed adjusted for the TC traveling speed. The MSLP calculated by Eq. (9) is smaller than the MSLP calculated by the original method of Knaff and Zehr (2007), in which the WPR forcing factors are held constant. For comparison, another WPR with the same predictors as those of Knaff and Zehr (2007) is built based on the scatter data, using the following formula:

$$\mathrm{MSLP} = 4.744 - 0.757V_{\mathrm{srm}} - 0.016V_{\mathrm{srm}}^2 - 0.450S_{\mathrm{KZ}} - 0.342\varphi + P_{\mathrm{env}}. \tag{10}$$

Kieu et al. (2010) suggested a statistical WPR, with two additional items relative to those employed by the Knaff and Zehr (2007) WPR. The regression coefficients are obtained from the aircraft datasets, which are created as

TABLE 1. Summary of the statistics associated with the WPR models for the dependent and independent datasets. MAE is the mean absolute error from observations, Bias is defined as the bias from observations, and RMSE is the root-mean-square error. The MAE values are statistically different than those produced by the KZ07-scattered WPR and are shown in italics where the difference is significant at the 99% level.

Data	WPR model	MAE	Bias	RMSE
Dependent data (1965–85)	Atkinson and Holliday (1977) (AH)	*9.81*	*2.88*	*13.24*
	Dvorak (1984)	*11.69*	*8.87*	*15.76*
	Koba et al. (1991)	*11.00*	*5.97*	*14.66*
	CMA (Ying et al. 2014)	*9.76*	*1.99*	*13.10*
	KZ07-binned	*10.78*	*2.83*	*14.43*
	KZ07-scattered	9.22	0.00	12.45
	Kieu et al. (2010)	9.27	0.00	12.43
	Chavas et al. (2017)	9.70	0.00	12.77
Independent data (1986–87)	Atkinson and Holliday (1977)	*11.95*	*6.99*	*15.09*
	Dvorak (1984)	*15.67*	*13.83*	*19.74*
	Koba et al. (1991)	11.16	0.07	13.73
	CMA (Ying et al. 2014)	*11.72*	*6.09*	*14.80*
	KZ07-binned	*13.28*	*4.95*	*16.60*
	KZ07-scattered	11.05	2.48	14.14
	Kieu et al. (2010)	11.05	4.56	14.11
	Chavas et al. (2017)	*11.44*	*2.48*	*14.36*

$$\begin{aligned}\mathrm{MSLP} = {} & 3.386 - 0.013V_{\mathrm{srm}}^2 - 0.62V_{\mathrm{srm}} - 0.32\varphi \\ & - 0.171S_{\mathrm{KZ}} - 0.17\frac{\partial V_{\mathrm{srm}}}{\partial t} + 0.053\frac{\partial V_{\mathrm{srm}}}{\partial t} \times S_{\mathrm{KZ}} \\ & - 0.014V_{\mathrm{srm}} \times S_{\mathrm{KZ}} + P_{\mathrm{env}}. \end{aligned} \tag{11}$$

Chavas et al. (2017) demonstrate that the central pressure deficit depends on two variables: MSW and half the product of the Coriolis parameter f and outer storm size S_8. The WPR was developed as follows:

$$\mathrm{MSLP} = -1.50V_{\mathrm{srm}} - 0.17\left(\frac{1}{2}fS_8\right) + 10.05 + P_{\mathrm{env}}. \tag{12}$$

The potential fitting capabilities of these WPRs in terms of the MAE, the bias, and the root-mean-square error (RMSE) from observations are estimated from the dependent and independent data (Table 1). The MSLP from observations and those calculated based on these WPR models are shown in Fig. 8. These statistical WPR equations [Eqs. (9)–(12)] are abbreviated to KZ-binned WPR, KZ-scattered WPR, Kieu WPR, and Chavas WPR, respectively. It must be noted that these functions aren't the original WPRs in their papers, but adopted the predictors suggested by them. The regression coefficients were obtained based on the aircraft datasets. The results show that there are substantial improvements in the KZ-scattered WPR [Eq. (10)] and Kieu WPR [Eq. (11)] over the other relationships. The KZ-scattered WPR explains 71% of the variance with a MAE of 9.21 hPa. The errors produced by Eqs. (10) and (11) are similar, which means inclusion of these two items $[(\partial V_{\mathrm{srm}}/\partial t) \times S_{\mathrm{KZ}}$ and $V_{\mathrm{srm}} \times S_{\mathrm{KZ}}]$ as additional predictors did not improve the WPR model.

The error statistics that are statistically different (99% level) to those produced by KZ-scattered include the KZ-binned WPR, AH WPR, Dvorak WPR, and Koba WPR (Tabel 1). Applications of the latter three WPRs lead to an overestimation of the MSLP, particularly for that of Dvorak (1975), with a MAE of 11.69 hPa and a bias of 8.87 hPa. The overestimation of MSW by Dvorak technique is supported by Harper (2002), particularly for intense TCs (Holland 2008). This result also shows the improvement by adding these factors (TC size, latitude, translation speed, and environmental pressure) into the statistical WPRs, which is consistent with the results of Knaff and Zehr (2007).

The WPR table used by CMA performed equivalently with AH WPR, which was used to assign MSW in JTWC since 1978 (U. S. Fleet Weather Facility 1978). The CMA WPR table and AH WPR performed better than Dvorak and Koba WPR. Compared to KZ-scattered WPR, MSLP-AH is a little higher for weak TCs (MSW $\leqq$ 40 m s^{-1}). The WPR of Chavas et al. (2017) seems also good for the dependent data, with a MAE of 9.66 hPa and a RSME of 12.80, which is not statistically different from those produced by the KZ-scattered WPR.

After MSW in the Koba WPR converted to 1-min mean wind speed, based on the ratio suggested by Atkinson (1974), the MSLP values are largest for TCs weaker than 30 m s^{-1}, and smaller than MSLP-Dvorak for TCs with intensity between 30 and 55 m s^{-1} (Fig. 8).

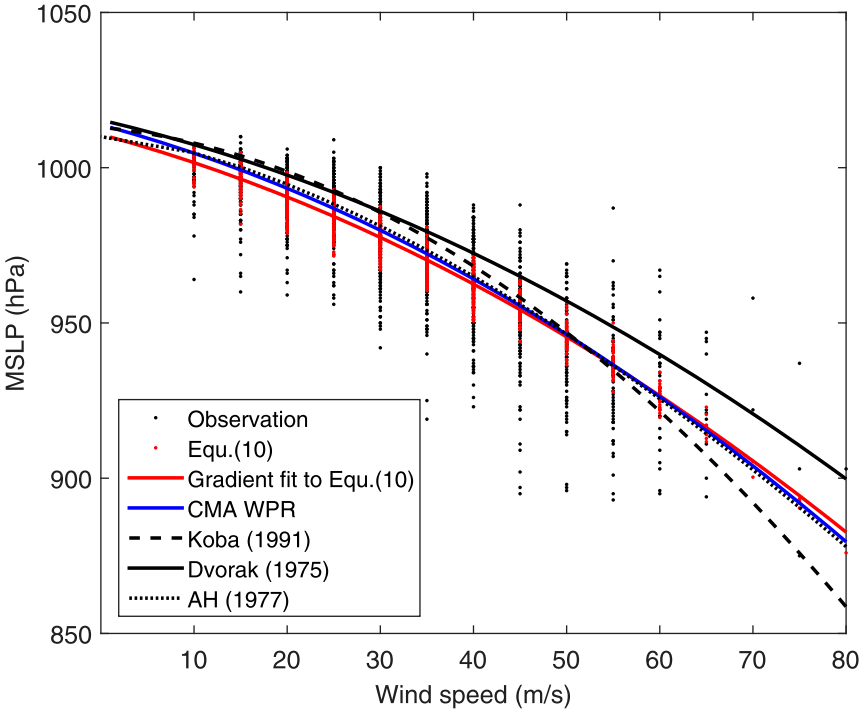

FIG. 8. MSLP from observations and calculated based on wind–pressure models [Eq. (10)]. Also shown are the relationships proposed by Dvorak (1975), Atkinson and Holliday (1977), and Koba et al. (1991). The 10-min average wind speed of Koba et al. (1991) WPR is converted to 1-min average wind speed based on Atkinson (1974).

This distribution is consistent with the MSLP values based on RSMC best track data (Fig. 7). However, the MSLP-Koba is smallest for TCs stronger than 55 m s^{-1}.

An independent dataset from the 1986–87 TC seasons (i.e., 123 samples) is also used to evaluate the equations. The statistical results (Table 1, bottom) are consistent with those of the dependent dataset, which show that Eq. (10) performs the best with the WPR.

5. Factors effect on the wind–pressure relationship

Composites of the MSLP are constructed by binning the MFW into groups every 5 m s^{-1} for different factor-based stratifications to explore the linear effect of the factors on WPRs based on the dataset used. The number of cases for most groups with an MFW greater than 60 m s^{-1} is less than 10; therefore, these groups are combined with the 60 m s^{-1} group. Composites are shown in Fig. 9 and discussed in the following. The detailed mean statistics of the each stratification are shown in Table 2.

The average P_{env} of all the samples is 1008.7 hPa, with a standard deviation of 2.9 hPa, and a range of 998.2–1020.5 hPa. Composites were constructed for environmental pressure stratification higher or lower than 1008.7 hPa, resulting in 978 and 929 cases, respectively. It is shown that the WPR is clearly a function of P_{env} (Fig. 9a). The differences of the MSLP between the two environmental pressure stratifications appear somewhat systematic. For example, TCs with a larger P_{env} will have a higher value of MSLP for a given MFW. The MSLP will increase with increasing P_{env} because the pressure gradient force should remain constant when other forcing factors are held constant.

Koba et al. (1991) and Knaff and Zehr (2007) found that stable or weakening TCs tend to have lower pressures for intensities below 33 m s^{-1} and higher pressures above 33 m s^{-1}. Therefore, composites based on this type of intensification trend stratification are also constructed here (Fig. 9b). Overall, the trends for MSLP are similar to Koba et al. (1991) and Knaff and Zehr (2007); however, a threshold of 50 m s^{-1} is found here instead of 33 m s^{-1}.

The mean TC translation speed for all samples is 5.1 m s^{-1}, with a standard variance of 2.5 m s^{-1}. The composites of TC translation speed larger and smaller than 5.1 m s^{-1} (Fig. 9c) show that TCs traveling faster will on average have a larger MFW for a given MSLP. This is consistent with the finding of previous studies that TCs with higher speeds have a slightly

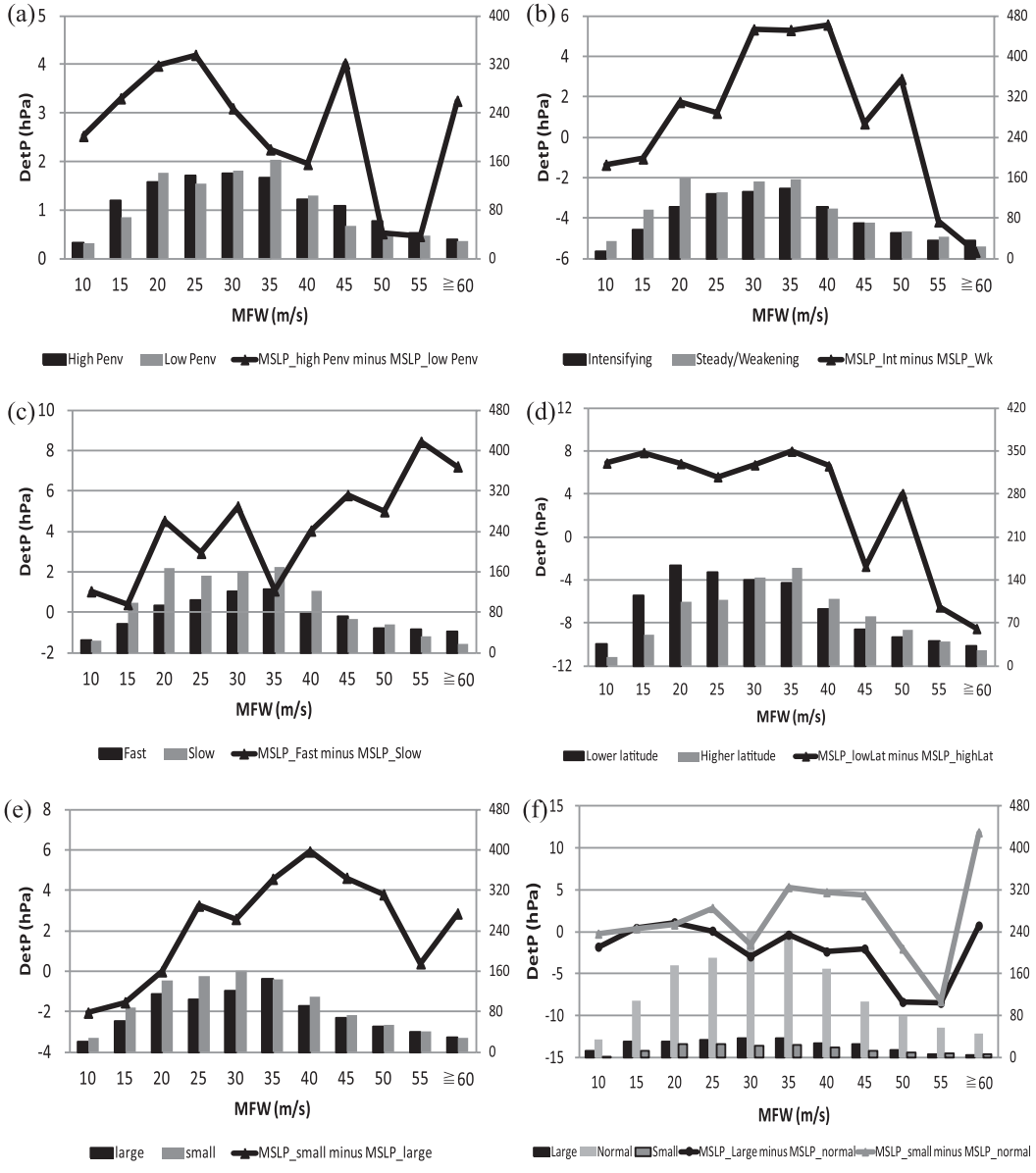

FIG. 9. Composites of DetP vs MSW for (a) two environmental pressure–based stratifications, (b) two intensity change–based stratifications, (c) two translation speed–based stratifications, (d) two latitudinal stratifications, (e) two S_8-based stratifications, and (f) three S_{KZ}-based stratifications. The solid lines indicate the value of MSLP (left y axis), and the bars indicate the numbers of each group (right y axis).

larger intensity (Schwerdt et al. 1979) and MFW (Mueller et al. 2006). The largest difference from this stratification occurs when the MFW is greater than 55 m s^{-1}.

The mean latitude for all samples is 19.2°N from a range of 4.0° to 43.6 °N. Composites are constructed for samples equatorward and northward of 19.2°N, resulting in 1012 and 895 cases, respectively. The shapes of these curves (Fig. 9d) show that in most cases TCs with equal MFW have a lower MSLP when they are located at higher latitude. However, unlike the previous results (Knaff and Zehr 2007), this relationship between the WPR and latitude only holds for samples with an MFW $\leq$ 45 m s^{-1}, and the opposite occurs for an MFW $>$ 45 m s^{-1}. This suggests that TCs at higher latitude show a tendency of a lower MSLP for intensities $\leq$ 45 m s^{-1}, and a higher MSLP above this threshold. To explore the reason, the translation speed (SPD) and the intensity change (Vt) were calculated by binning the MFW into groups every 5 m s^{-1} for different latitude-based stratifications (Fig. 10). The result shows that the

TABLE 2. Mean statistics of the individual stratification. TC latitude is denoted by φ, TC size is denoted by S_{KZ}, environmental pressure is denoted by P_{env}, and V_{srm} is the maximum wind speed (MSW) adjusted for the TC traveling speed (SPD), S_8 is the radius of 8 m s^{-1}, and S_{KZ} is the TC size suggested by Knaff and Zehr (2007).

Samples	No.	Avg φ (°N)	Avg S_8 (km)	Avg S_{KZ}	Avg MSW (m s^{-1})	Avg P_{env} (hPa)	Avg SPD (m s^{-1})	Avg MSLP (hPa)
Whole	1874	19.23	520.18	0.45	29.41	1008.73	5.12	972.80
<19.23°N	884	13.85	505.32	0.46	28.18	1009.17	4.96	976.42
≥19.23°N	990	25.19	536.73	0.44	30.81	1008.16	5.29	967.35
Fast	823	19.47	522.60	0.44	30.76	1008.91	7.41	971.83
Slow	1051	18.96	518.29	0.46	28.38	1008.58	3.36	972.40
Small	278	18.54	462.58	0.31	26.92	1008.48	4.84	976.85
Avg	1304	19.27	505.47	0.45	29.45	1008.67	5.11	972.00
Large	292	18.79	644.95	0.47	29.96	1008.93	5.25	971.65
Weakening/steady	1011	21.44	518.08	0.44	28.38	1008.54	5.08	972.79
Intensifying	863	16.43	522.64	0.46	30.67	1008.93	5.17	971.38

high-latitude cases move significantly faster than lower-latitude cases when MFW is larger than 45 m s^{-1}, which make the MFW larger for high-latitude samples with the same MSLP. Meanwhile, the mean values of Vt for the high-latitude cases are between −0.1 and 1.3 m s^{-1}, while those for the low-latitude cases are between 0.9 and 5.2 m s^{-1}. As discussed above, the stable or weakening samples tend to have lower pressures for weaker TCs and higher pressures for strong TCs, which make the TCs tend to have a higher MSLP for high-latitude samples with a given MFW.

Two types of TC size (i.e., S_8 and S_{KZ}) are tested in this study. The mean value of S_8 is 514.1 km. The composites of S_8 constructed for samples larger or smaller than 514.1 km are shown in Fig. 9e. The large (small) TCs tend to have a lower (higher) MSLP for a given MFW, when MFW exceeds 20 m s^{-1}. The largest difference of the MSLP between large and small TCs is 5.9 hPa when the MSW is 40 m s^{-1}.

Following Knaff and Zehr (2007), three composites for the S_{KZ} are constructed (Fig. 9f). Large and small cases denote cases greater and less than 1 standard deviation from the mean, respectively, and average cases lie within the range of the mean ±1 standard deviation. The mean value of S_{KZ} is 0.45, with a standard variance of 0.29, which is similar to values (0.49

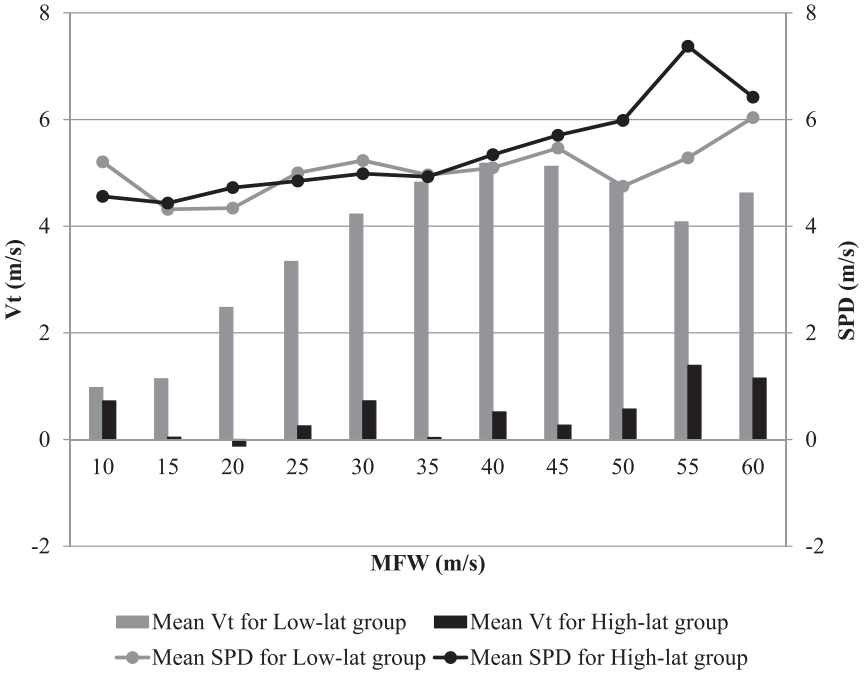

FIG. 10. Composites of the mean intensification trend (Vt) and translation speed (SPD) vs MFW for higher-latitude and lower-latitude stratifications. The bars indicate the value of Vt (left y axis), and the solid lines indicate the value of SPD (right y axis).

TABLE 3. Error statistics associated with the sequential addition of each predictor to the WPR models. Each calculation is adjusted to zero mean bias. Pressure deficit is denoted by Δp, latitude is denoted by φ, TC size is denoted by S_{KZ}, and V_{srm} is the maximum wind speed (MSW) adjusted for the TC traveling speed. MAE is the mean absolute error from observations, and RMSE is the root-mean-square error.

		Dependent data (1965–85)		Independent data (1986–87)	
Dependent variable	Predictor	MAE	RMSE	MAE	RMSE
MSLP	MSW	9.94	13.01	11.46	14.26
	V_{srm}	9.88	12.92	11.51	14.29
	V_{srm}^2	9.82	12.98	11.32	14.32
	V_{srm}^2, V_{srm}	9.68	12.75	11.28	14.13
Δp	V_{srm}^2, V_{srm}	9.57	12.69	11.22	14.15
	V_{srm}^2, V_{srm}, φ	9.27	12.49	11.10	14.21
	V_{srm}^2, V_{srm}, φ, S_{KZ}	9.22	12.45	11.05	14.14
	V_{srm}^2, V_{srm}, φ, S_{KZ}, $\partial V_{srm}/\partial t$	9.22	12.45	11.03	14.10
	V_{srm}^2, V_{srm}, φ, S_{KZ}, $\partial V_{srm}/\partial t$, $(\partial V_{srm}/\partial t) \times S_{KZ}$	9.28	12.44	11.06	14.12
	V_{srm}^2, V_{srm}, φ, S_{KZ}, $\partial V_{srm}/\partial t$, $(\partial V_{srm}/\partial t) \times S_{KZ}$, $V_{srm} \times S_{KZ}$	9.27	12.43	11.05	14.11

and 0.22, respectively) found in Knaff and Zehr (2007). Differences between the three composites are minimal for cases less than 30 m s^{-1}. For cases with an MFW larger than 30 m s^{-1}, the MSLP of small TCs tend to be significantly larger than that of average and large TCs, except for the MFW 50 m s^{-1} group. Overall, small TCs tend to have a higher MSLP for most cases based on both S_8 and S_{KZ}.

Table 3 shows the error statistics arising from the sequential addition of each predictor to the WPR. Each model is adjusted to zero mean bias. The predictor selection procedure found the MSW^2 to be the most important factor in the WPR model. Based on the gradient wind balance [Eq. (5)], MSW^2 represents the centrifugal effect and outweighs the Coriolis forcing in the TC inner core. This indicates that the tangential flows in the TC inner core can be approximated by the cyclostrophic relation, consistent with the theoretical result of previous studies (Takahashi 1939; 1952; Fortner 1958; Atkinson and Holliday 1977; Love and Murphy 1985). Meanwhile, the latitude produces the greatest improvement, with small additional improvements from the translational speed and the environmental pressure. However, the TC size and intensity change added nearly no skill in the WPR equation. The negligible contribution from the intensity change was also noted by Knaff and Zehr (2007) and Holland (2008). For example, Knaff and Zehr (2007) found that the differences in the WPRs between intensifying and weakening TCs were due more to differences in TC size and latitude.

6. Summary

The WPRs for TCs in the western North Pacific are reexamined based on aircraft data, CMA best track data, and daily JRA-55 data during 1957–87. The MSLP was estimated from aircraft reconnaissance, and MSW were adjusted from the maximum wind speed at the flight level (MFW) by multiplying them with the recommended ratio suggested by Franklin et al. (2003).

The WPRs based on aircraft observations with that based on the best track datasets (CMA and RSMC-Tokyo) are compared. Results show that the WPR for the CMA dataset during the 1965–87 is more close to the observation-based WPR, while the MSLP for 1955–64 are much higher based on CMA datasets for each wind group. This indicates that there was a systematic wind speed bias (two high) before 1965 in the CMA best track dataset. The most important reason is that the mean aircraft based MSLP was higher during 1957–64 than during 1965–87 for each MSW group, since the onboard aircraft and observational instruments were upgraded around 1965. Aircraft reconnaissance data played a role in estimating MSW during the period in the best track datasets. Further analyses found that the WPR table used by CMA after 1972 is similar with AH WPR, which results the mean MSLP in the CMA best track dataset higher than MSLP-AR for weak TCs, but very close for strong TCs (MSW $\geq$ 35 m s^{-1}). Meanwhile, the WPR in the RSMC dataset is better for weak TCs (MSW $\leq$ 35 m s^{-1}) after the MSW-RSMC converted by Dvorak conversion table (1984), when using the aircraft datasets during 1977–87 as a baseline.

Several prevailing operational WPRs used in WNP are reexamined here, which include the WPRs suggested by Dvorak (1975), Koba et al. (1991), Atkinson and Holliday (1977), Knaff and Zehr (2007), and the WPR used by CMA (Ying et al. 2014). Some other WPRs suggested based on the physical understanding recently, which include WPRs derived by Kieu et al. (2010), and Chavas et al. (2017). The results show that there are substantial improvements in the KZ-scattered

TABLE A1. Mean statistics of the individual composites.

Samples	No.	Avg φ	Avg S_{KZ}	Avg MSW	Avg P_{env}	Avg SPD	Avg MSLP
Whole	1874	19.23	0.45	29.41	1008.73	5.12	972.80
<20°N	1063	14.33	0.46	28.02	1009.14	4.90	976.55
20°–30°N	674	24.43	0.43	30.60	1008.06	4.91	966.84
>30°N	137	32.58	0.55	29.89	1008.77	7.43	973.08
Small	160	19.42	0.15	30.50	1008.96	5.15	973.08
Avg	1460	19.14	0.42	29.07	1008.67	5.05	972.69
Large	254	20.11	1.01	28.28	1008.89	5.29	973.28

WPR [Eq. (10)] over the other relationships. The coefficients of each variable of KZ-scattered WPR are obtained based on the aircraft datasets, which are different from the original Knaff and Zehr (2007) WPR. MSLP calculated by Eq. (10) is smaller than that calculated by original Knaff and Zehr (2007) WPR when the forcing factors are held same. The KZ-scattered WPR explains 71% of the variance with a MAE of 9.21 hPa. The errors produced by Eq. (10) and Kieu WPR [Eq. (11)] are almost equal, which means inclusion of these two items $[(\partial V_{srm}/\partial t) \times S$ and $V_{srm} \times S]$ as additional predictors didn't improve the WPR model.

The effects of TC center latitude, size, translation speed, intensification trend, and environmental pressure latitude on the WPRs were examined. The results show that fast-traveling TCs, small in size and located in high environmental pressure at low latitudes tend to have a higher MSLP for a given MSW. Meanwhile, the latitude produces the greatest improvement, with small additional improvements from the translational speed and the environmental pressure. However, the TC size and intensity change added only a little skill in the WPR equation.

Acknowledgments. We thank Dr. John Knaff and the other two anonymous reviewers for their diligent efforts and constructive comments, which helped improve this manuscript. This research was supported jointly by the Key Program for International S&T Cooperation Projects of China 2017YFE0107700, and the National Natural Science Foundation of China Grants 41405060, 41475060, 41475082, and 41775065.

APPENDIX

Procedure of Knaff and Zehr (2007) Wind–Pressure Relationship Repeated

The samples are divided into different groups. Three latitude-based composites consist of equatorward of 20° latitude, between 20° and 30° latitude, and northward of 30° latitude. Three size-based composites are constructed from those cases less than 1 standard deviation from the mean (small), between +1 and −1 standard deviation from the mean (average), and those cases with sizes greater than 1 standard deviation from the mean (large). Individual composites are created by binning the MSW every 4.5 m s^{-1}. The mean statistics of the individual composites are shown in Table A1. The composite averages of each of the individual composites are used to create one unifying regression equation that can be used to predict Δp as a function of the MSW, latitude, and size. The WPR is created as follows:

$$\mathrm{MSLP} = 8.086 - 0.600V_{srm} - 0.012V_{srm}^2 - 3.18S - 0.166\varphi + P_{env}, \quad \text{(A1)}$$

where notations follow Knaff and Zehr (2007).

REFERENCES

Atkinson, G. D., 1974: Investigation of gust factors in tropical cyclones. FLEWEACEN Tech. Note JTWC 74-1, Fleet Weather Center, Guam, 9 pp.

——, and C. R. Holliday, 1977: Tropical cyclone minimum sea level pressure/maximum sustained wind relationship for the western North Pacific. *Wea. Forecasting*, **105**, 421–427, https://doi.org/10.1175/1520-0493(1977)105<0421:TCMSLP>2.0.CO;2.

Black, P. G., 1993: Evolution of maximum wind estimates in typhoons. *Tropical Cyclone Disasters*: *Proceedings of ICSU/WMO International Symposium*, J. Lighthill et al., Eds., Peking University Press.

Chavas, D. R., K. A. Reed, and J. A. Knaff, 2017: Physical understanding of the tropical cyclone wind-pressure relationship. *Nat. Commun.*, **8**, 1360, https://doi.org/10.1038/s41467-017-01546-9.

Courtney, J., and J. A. Knaff, 2009: Adapting the Knaff and Zehr wind-pressure relationship for operational use in tropical cyclone warning centers. *Aust. Meteor. Oceanogr. J.*, **58**, 167–179, https://doi.org/10.22499/2.5803.002.

Dvorak, V. F., 1975: Tropical cyclone intensity analysis and forecasting from satellite imagery. *Mon. Wea. Rev.*, **103**, 420–430, https://doi.org/10.1175/1520-0493(1975)103<0420:TCIAAF>2.0.CO;2.

——, 1984: Tropical cyclone intensity analysis using satellite data. NOAA Tech. Rep. NESDIS 11, NOAA, 45 pp.

Fortner, L. E., Jr., 1958: Typhoon Sarah, 1956. *Bull. Amer. Meteor. Soc.*, **39**, 633–639, https://doi.org/10.1175/1520-0477-39.12.633.

Franklin, J. L., M. L. Black, and K. Valde, 2003: GPS dropwindsonde wind profiles in hurricanes and their operational

implications. *Wea. Forecasting*, **18**, 32–44, https://doi.org/10.1175/1520-0434(2003)018<0032:GDWPIH>2.0.CO;2.

Grocott, D. G., 1963: Doppler correction for surface movement. *J. Inst. Navig.*, **16**, 57–63, https://doi.org/10.1017/S0373463300018476.

Harper, B. A., 2002: Tropical cyclone parameter estimation and the Australian region: Wind–pressure relationships and related issues for engineering planning and design. Systems Engineering Australia Rep. J0106-PR003E, 92 pp.

Henderson, R. S., 1978: USAF aerial weather reconnaissance using the Lockheed WC-130 aircraft. *Bull. Amer. Meteor. Soc.*, **59**, 1136–1143, https://doi.org/10.1175/1520-0477(1978)059<1136:UAWRUT>2.0.CO;2.

Holland, G., 2008: A revised hurricane pressure–wind model. *Mon. Wea. Rev.*, **136**, 3432–3445, https://doi.org/10.1175/2008MWR2395.1.

Kieu, C. Q., H. Chen, and D.-L. Zhang, 2010: An examination of the pressure–wind relationship for intense tropical cyclones. *Wea. Forecasting*, **25**, 895–907, https://doi.org/10.1175/2010WAF2222344.1.

Knaff, J. A., and C. R. Sampson, 2006: Reanalysis of west Pacific tropical cyclone intensity 1966-1987. *27th Conf. on Hurricanes and Tropical Meteorology*, Monterey, CA, Amer. Meteor. Soc., 5B.5, https://ams.confex.com/ams/27Hurricanes/techprogram/paper_108298.htm.

——, and R. M. Zehr, 2007: Reexamination of tropical cyclone wind–pressure relationships. *Wea. Forecasting*, **22**, 71–88, https://doi.org/10.1175/WAF965.1.

Knapp, K. R., and M. C. Kruk, 2010: Quantifying interagency differences in tropical cyclone best-track wind speed estimates. *Mon. Wea. Rev.*, **138**, 1459–1473, https://doi.org/10.1175/2009MWR3123.1.

——, J. A. Knaff, C. R. Sampson, G. M. Riggio, and A. D. Schnapp, 2013: A pressure-based analysis of the historical western North Pacific tropical cyclone intensity record. *Mon. Wea. Rev.*, **141**, 2611–2631, https://doi.org/10.1175/MWR-D-12-00323.1.

Koba, H., T. Hagiwara, S. Osano, and S. Akashi, 1991: Relationships between CI number and minimum sea level pressure / maximum wind speed of tropical cyclones. *Geophys. Mag.*, **44**, 15–25.

Laseur, N. E., and H. F. Hawkins, 1963: An analysis of Hurricane Cleo (1958) based on data from research reconnaissance aircraft. *Mon. Wea. Rev.*, **91**, 694–709, https://doi.org/10.1175/1520-0493(1963)091<0694:AAOHCB>2.3.CO;2.

Love, G., and K. Murphy, 1985: The operational analysis of tropical cyclone wind fields in the Australian northern region. Bureau of Meteorology, Northern Territory Region, Research Papers, 1984-85 (Nov), 44–51.

Mueller, K. J., M. DeMaria, J. A. Knaff, J. P. Kossin, and T. H. Vonder Haar, 2006: Objective estimation of tropical cyclone wind structure from infrared satellite data. *Wea. Forecasting*, **21**, 990–1005, https://doi.org/10.1175/WAF955.1.

Neumann, C. J., 1952: Wind estimations from aerial observations of sea conditions. Weather Squadron Two, NAS Jacksonville, 29 pp., http://www.aoml.noaa.gov/hrd/hurdat/seastate-aircraft.pdf.

Nolan, D. S., J. A. Zhang, and E. W. Uhlhorn, 2014: On the limits of estimating the maximum wind speeds in hurricanes. *Mon. Wea. Rev.*, **142**, 2814–2837, https://doi.org/10.1175/MWR-D-13-00337.1.

Operational Department of China Central Meteorological Administration, Ed., 1980: *Reference Manual on Typhoon Reconnaissance Report and Warning Message* (in Chinese). China Meteorological Press, 117 pp.

Schwerdt, R. W., F. P. Ho, and R. R. Watkins, 1979: Meteorological criteria for standard project hurricane and probable maximum hurricane wind fields—Gulf and East Coasts of the United States. NOAA Tech. Rep. NWS 23, NOAA, 317 pp.

Song, J.-J., Y. Wang, and L. Wu, 2010: Trend discrepancies among three best track data sets of western North Pacific tropical cyclones. *J. Geophys. Res.*, **115**, D12128, https://doi.org/10.1029/2009JD013058.

Takahashi, K., 1939: Distribution of pressure and wind in a typhoon. *J. Meteor. Soc. Japan, Ser. 2*, **17**, 417–421.

——, 1952: Techniques of the typhoon forecast. *Geophys. Mag.*, **24**, 1–8.

Uhlhorn, E. W., and D. S. Nolan, 2012: Observational understanding in tropical cyclones and implications for estimated intensity. *Mon. Wea. Rev.*, **140**, 825–840, https://doi.org/10.1175/MWR-D-11-00073.1.

U.S. Fleet Weather Facility, 1965: Annual Tropical Storm Report. U.S. Fleet Weather Facility, Miami, FL, 258 pp.

——, 1978: Annual Tropical Storm Report. U.S. Fleet Weather Facility, Miami, FL, 177 pp.

——, 2007: Annual Tropical Storm Report. U.S. Fleet Weather Facility, Miami, FL, 124 pp.

Velden, C., and Coauthors, 2006: The Dvorak tropical cyclone intensity estimation technique: A satellite-based method that has endured for over 30 years. *Bull. Amer. Meteor. Soc.*, **87**, 1195–1210, https://doi.org/10.1175/BAMS-87-9-1195.

Weatherford, C. L., and W. M. Gray, 1988: Typhoon structure as revealed by aircraft reconnaissance. Part I: Data analysis and climatology. *Mon. Wea. Rev.*, **116**, 1032–1043, https://doi.org/10.1175/1520-0493(1988)116<1032:TSARBA>2.0.CO;2.

Willoughby, H. E., 1990: Gradient balance in tropical cyclones. *J. Atmos. Sci.*, **47**, 265–274, https://doi.org/10.1175/1520-0469(1990)047<0265:GBITC>2.0.CO;2.

——, and M. E. Rahn, 2004: Parametric representation of the primary hurricane vortex. Part I: Observations and evaluation of the Holland (1980) model. *Mon. Wea. Rev.*, **132**, 3033–3048, https://doi.org/10.1175/MWR2831.1.

——, J. Masters, and C. Landsea, 1989: A record minimum sea level pressure observed in Hurricane Gilbert. *Mon. Wea. Rev.*, **117**, 2824–2828, https://doi.org/10.1175/1520-0493(1989)117<2824:ARMSLP>2.0.CO;2.

Ying, M., W. Zhang, H. Yu, X. Q. Lu, J. X. Feng, Y. X. Fang, Y. T. Zhu, and D. Q. Chen, 2014: An overview of the China Meteorological Administration tropical cyclone database. *J. Atmos. Oceanic Technol.*, **31**, 287–301, https://doi.org/10.1175/JTECH-D-12-00119.1.